

Estimation of the Deforestation Through the Forest Canopy Density Model Derived From Remote Sensing

Pathirathna S.M.R.A.^{1*}, Ranasinghe A.K.R.N.², and Bandara H.R.S.³

¹ Lecturer, Institute of Surveying and Mapping, Survey Department of Sri Lanka

² Snr Lecturer, Faculty of Geomatics, Sabaragamuwa University of Sri Lanka

³ Professor, Faculty of Geomatics, Sabaragamuwa University of Sri Lanka

*smadushar@gmail.com

Abstract : Forest degradation and deforestation are major concerns for governments worldwide. In Sri Lanka, the topic of deforestation, particularly concerning the Wilpattu Forest Complex, has been a significant point of discussion among environmentalists and the general public. This study offers a scientific perspective on this issue by assessing periodic changes in land cover within the controversial area of Wilpattu Forest using satellite data. Forest canopy changes in the Wilpattu Forest area from 1988 to 2023 were identified by developing Forest Canopy Density (FCD) models. These models were generated for the years 1988, 1992, 2001, 2010, 2015, 2018, 2020, and 2023. The FCD models were created using Vegetation Density and Scale Shadow Indexes. Vegetation Density was determined using the Advanced Vegetation Index (AVI) and Bare Soil Index (BSI), while the Scale Shadow Index was derived from the Shadow Index and Thermal Index. The FCD models were classified into five categories: High FCD, Low FCD, scrub, grassland, and bare land. A comparative analysis of these categories across different years provided insights into land cover changes. Further analysis at the Divisional Secretariat (DS) and Grama Niladhari (GN) division levels was conducted by overlaying their shapefiles onto the FCD models. The results revealed significant land use changes between 2010 and 2018, including the conversion of forest areas into residential, road, or farmland purposes. This indicates that land use changes were driven not only by deforestation but also by forest degradation. However, from 2018 to 2020, the forest showed resilience with no evidence of deforestation. In conclusion, the study highlights that land use changes in the Wilpattu Forest Complex result from both deforestation and forest degradation. The observed resilience from 2018 to 2020 underscores the dynamic nature of the forest ecosystem, providing essential insights for informed discussions and policymaking on forest conservation in Sri Lanka.

Keywords: Forest Canopy Density models, Deforestation, Wilpattu Forest, Vegetation Density, Scale Shadow Index

1 Introduction

Forest degradation and deforestation are critical concerns for governments worldwide. Deforestation refers to the conversion of forests to non-forest uses, such as agriculture and large-scale construction, while forest degradation occurs when forest ecosystems lose their ability to provide essential goods and services to both people and the environment. According to the International Union for Conservation of Nature (IUCN), more than 50% of tropical forests have been destroyed since 1960. The increasing pressure from deforestation and forest degradation poses severe threats to biodiversity and human livelihoods. Therefore,

monitoring these processes and implementing effective management strategies to preserve and enhance forest cover is crucial (Aranha et al., 2008; Bevenivk et al., 2016; IUCN, 2019).

In Sri Lanka, deforestation has been a topic of significant debate, particularly concerning the Wilpattu Forest Complex (WFC). While environmentalists and the general public have raised concerns about deforestation in this region, particularly in mass media, there is often a lack of scientific data underpinning these discussions. A major point of contention revolves around the government's efforts to clear large tracts of land in the WFC for the resettlement of people displaced by the country's three-decade civil war. Government officials argue that the resettlement is taking place in areas that were previously established as villages before the conflict. Identifying the timing and location of changes in forest cover within the Wilpattu Forest Complex is thus of great importance.

Forest Canopy Density (FCD) models provide a powerful tool for monitoring forest canopy cover and detecting changes over time. By utilizing satellite imagery and other remote sensing data, FCD models allow for accurate quantification of forest canopy extent and density with high spatial and temporal resolution. Since its introduction by Rikimaru in 1996 using Landsat TM data, the FCD model has been widely adopted in tropical forest studies to assess deforestation, forest health, afforestation, and other forest-related metrics (Rikimaru, 1996).

1.1 Objective

The study aims to assess periodic land cover changes within the contentious Wilpattu Forest Complex using satellite data, with a focus on the development and application of FCD models.

1.2 Study area

The Wilpattu forest complex is spread within North, North Central and North Western provinces in Sri Lanka and is fallen between $8^{\circ}16'59.82''$ – $8^{\circ}48'5.96''$ N Latitudes and $79^{\circ}54'0.37''$ – $80^{\circ}15'11.75''$ E Longitudes. From Northern direction it is border to "AruviAru" river. It has a border with the eastern coast from the East direction and the "Kala Oya" from the South direction. The Wilpattu forest complex has nine adjacent forest reserves and it is approximately 183 km away from the capital city of Colombo. The forest complex includes

tropical dry mixed evergreen forest, tropical thorny forest, riverine forest, dry grasslands, wetlands and coastal villus(Weerakoon and Goonatilake, 2007; "Wilpattu National Park," n.d.).

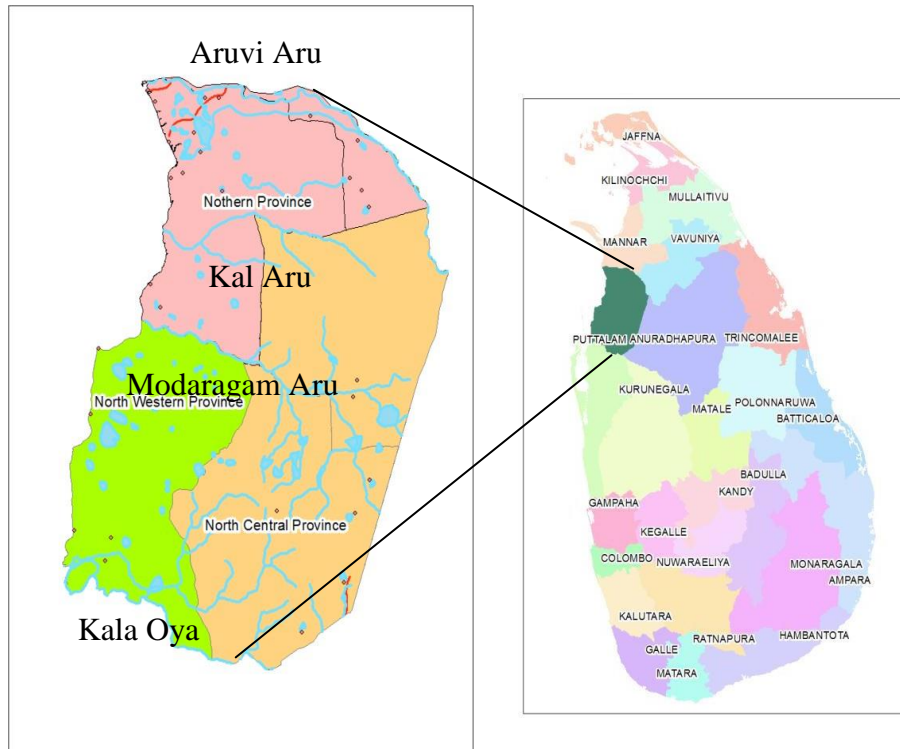


Figure 1: Wilpattu Forest Complex - Study Area.

1.3 Data used

The primary data used in this research was the satellite images of Landsat 5 - Thematic Mapper and Landsat 8 Operational Land Imager (OLI). The standard level-one terrain-corrected L1T images those geometrically calibrated and ortho-rectified to WGS-84 datum (zone 44N) were selected except the images of the Landsat. The limited number of least cloud disturbance images was available and selected due to heavy cloud disturbances in the optical images of the study area. The Landsat 7 images were not incorporated for this study due to strip error occurred in these images. All the optical satellite images and Digital Elevation Model were acquired free of charge from the United States Geological Survey (USGS) website. The Google Earth images were used for the purpose of visual interpretation. Demarcation and identification of the study area were carried out by using 1:50,000 topographic maps of the Survey Department of Sri Lanka. The table 3.1 shows the selected satellite images with details.

Table 1: Details of Satellite Images

Name of the Satellite	Date acquired the images
Landsat 5 (TM)	06 th Feb 1988, 01 th Feb1992, 09 th Feb 2001, 03 th March 2009 and, 18 th Feb 2010, 09 th March 2011
Landsat 8 (OLI)	11 th Dec 2013, 20 th March 2015, 18 th July 2018, 2 nd April 2020, 12 th March 2024
Digital Elevation	SRTM1N08E079V3, SRTM1N08E080V3

2 Methodology

Image pre-processing were conducted prior to the main data analysis and consist of geometric correction, radiometric correction, and atmospheric corrections processes to enhance the qualitatively and quantitative understanding of image components. FLAASH, based on MODTRAN, is used in this study for atmospheric correction. The study further employs Minimum Noise Fraction (MNF) to reduce noise, improve image quality and smoothing noisy bands to enhance the accuracy.

The reflectance of the light varies with the ecological and other factors associated with the plants. The Vegetation Indices (VI) help the acquisition of these different ecological properties of plants through analyzing the Multi or Hyper spectral imagery bands from satellite and drone data. The spectral reflectance responses captured by the satellite imagery have high correlation with the carbon, nitrogen and water cycles (Chang et al., 2016; Xue et al., 2017). Different Indices may indicate wide range of plant characteristics. The Indices are help to improve the accuracy of Remote Sensing image classifications. Also the Indices help to enhance the spectral information and increase the difference between the classes of interest. All the above factors lead to increase in the quality of resulted Land Use and Land Cover Mapping (Ustuner et al., 2014). Basically the Indices provide two categories of information as; information about plant growth and health and the information about the land cover (mining, forest, bare soil, pasture, water surfaces, industrialetc.). This study incorporated the Vegetation Indices (VI) ;Vegetation Density, Advanced Vegetation Index (AVI), Bare Soil Index , Shadow Index and Scale Shadow Index in developing the Forest Canopy Density model (FCD).

2.1 Development of the Forest Canopy Density (FCD)

The first major step in this research is the development of the Forest Canopy Density (FCD) models for the study area. The FCD is derived by integrating the Vegetation Density (VD) and the Scale Shadow Index (SSI). This integration involves transforming these indices to reflect forest canopy density values accurately. Both VD and SSI are dimensionless and are expressed as percentage scales, facilitating their synthesis on corresponding scales and units (Rikimaru et al., 2002).

2.1.1 Vegetation Density (VD)

The VD is derived by combining the Advanced Vegetation Index (AVI) and the Bare Soil Index (BSI). These indices, which capture a wide range of canopy densities, are computed through the Tasseled Cap (TC) transformation. The TC algorithm, providing appropriate coefficients for Landsat 8 images, is used to estimate both AVI and BSI (Pladsrichuay et al., 2018). The linear transformation applied results in eigenvectors that generate the VD for Landsat 8, with eigenvalues of 90.16% and 86.90% respectively, as detailed by (Pladsrichuay et al. 2018):

$$VD = -0.99966 (BSI) - 0.02617(AVI) \text{ ----- (01)}$$

2.1.2 Bare Soil Index (BSI)

The BSI is formulated using medium infrared information from Landsat images to enhance bare soil areas, uncultivated lands, and vegetation with significant background response. This index helps assess forest land conditions along a continuum from high vegetation to exposed soil conditions by combining vegetation and bare soil indices (Rikimaru et al., 2002). Soil reflectance depends on various characteristics such as composition, moisture, and texture. The IR region of the spectrum shows low reflectance due to soil moisture absorption. The BSI is calculated as follows, with values ranging from 0 to 200 (Rikimaru et al., 2002; Banerjee et al., 2014):

$$BSI = \frac{(B(SWIR1)+ B(Red))- (B(NIR)+ B(blue))}{(B(SWIR1)+ B(Red))+ (B(NIR)+ B(blue))} * 100 + 100 \text{ ----- (02)}$$

$$(0 < BI < 200)$$

2.1.3 Advanced Vegetation Index (AVI)

The AVI characterizes the spectral response of green vegetation, particularly absorption and reflectance in remote sensing. It improves upon the Normalized Difference Vegetation Index (NDVI) by highlighting subtle differences in forest canopy density, using the power degree of the infrared response. The AVI, sensitive to forest density and vegetation classes, is calculated as follows (Azizia et al., 2008):

$$AVI = [(B4 + 1) * (256 - B3) * (B4 - B3)]^{1/3} \quad \text{----- (03)}$$

Here, Band 4 (B4) is Near Infrared (NIR) Top Of Atmosphere (TOA) reflectance, and Band 3 (B3) is Red TOA reflectance. AVI values range from -1 to +1, where values close to zero indicate no green vegetation, and values near +1 (0.8 to 0.9) indicate high green leaf density (Banerjee et al., 2014).

2.1.4 Scale Shadow Index (SSI)

The SSI combines the Shadow Index (SI) and the Thermal Index (TI). The SI, a relative value normalized for use with other parameters, integrates Vegetation Index (VI) values with SI values. SSI values range from 0 (lowest shadow value) to 100 (highest shadow value), obtained through a linear transformation of the SI (Rikimaru et al., 2002). The SSI distinctly differentiates vegetation in the canopy from ground vegetation, significantly improving the accuracy of data analysis.

2.1.5 Thermal Index(TI)

The relatively cool temperature within a forest accounts for two factors. One is the forest canopy's protective effect that blocks the energy from the sun and absorbs it. The other is leaf surface evaporation, thus mitigates warming. This effect is the basis of the formulation of the thermal index. The thermal infrared band TM data is the source of thermal information. (Rikimaru et al., 2002; Himayah et al., 2016). Temperature data then used to separating a soil and a non-tree shadow.

$$TI = \frac{K_2}{(\ln((\frac{K_1}{L\lambda}) + 1))} \quad \text{----- (04)}$$

2.1.6 Shadow Index(SI)

The three dimensional structure of a forest is one unique characteristic of the forest. The RS data are used to extract the forest structure information. The trees and plant arrangement pattern decides the shadow pattern of a forest. The Young forest has low value of Canopy Shadow Index compared to old natural forest shadow. The forest shadow characteristics are examined by utilizing (a) spectral information on the forest shadow itself and(b) thermal information on the forest influenced by shadow. The shadow index is formulated via extraction of the low radiance of visible bands (Banerjee et al., 2014; Rikimaru et al., 2002).

If the forest canopy is very dense, the relative strength of the shadow can't always display the satellite data. The Shadow Index (SI) is drawn up by eliminating the low radiation of the visible bands (Rikimaru et al., 2002).

$$SI = ((256-Blue) \times (256-Green) \times (256-Red))^{1/3} \text{-----}(05)$$

FCD models were developed for the years 1988, 1992, 2001, 2010, 2015, 2018, 2020, and 2024, and subsequently categorized into five classes: High FCD, Low FCD, Scrub Land, Grass Land, and Bare Land. Validation of the models was performed by comparing the 2018 FCD model with the collected ground truth data..

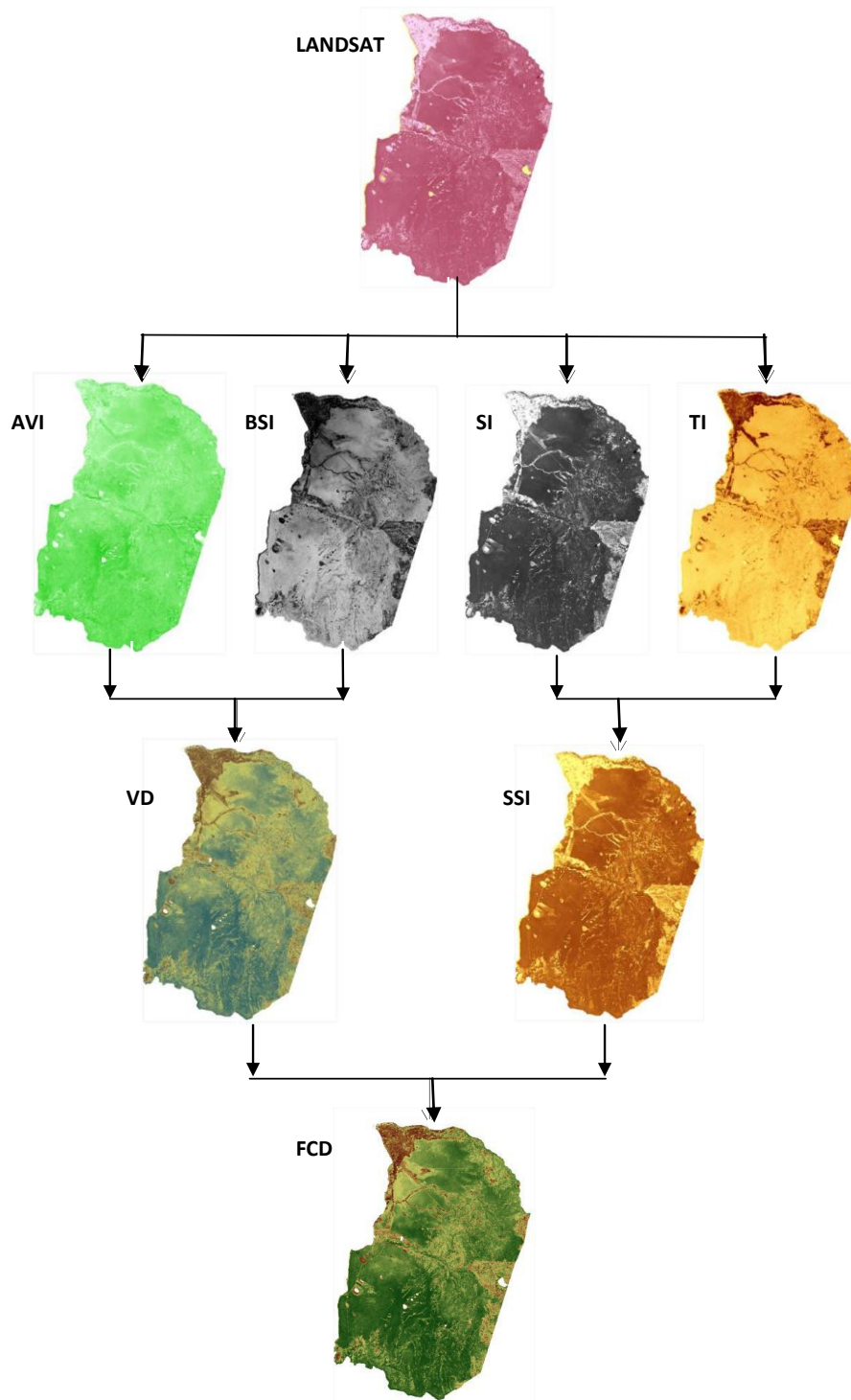


Figure 2.1: Generation of Forest Canopy Density by Utilizing Landsat Data.

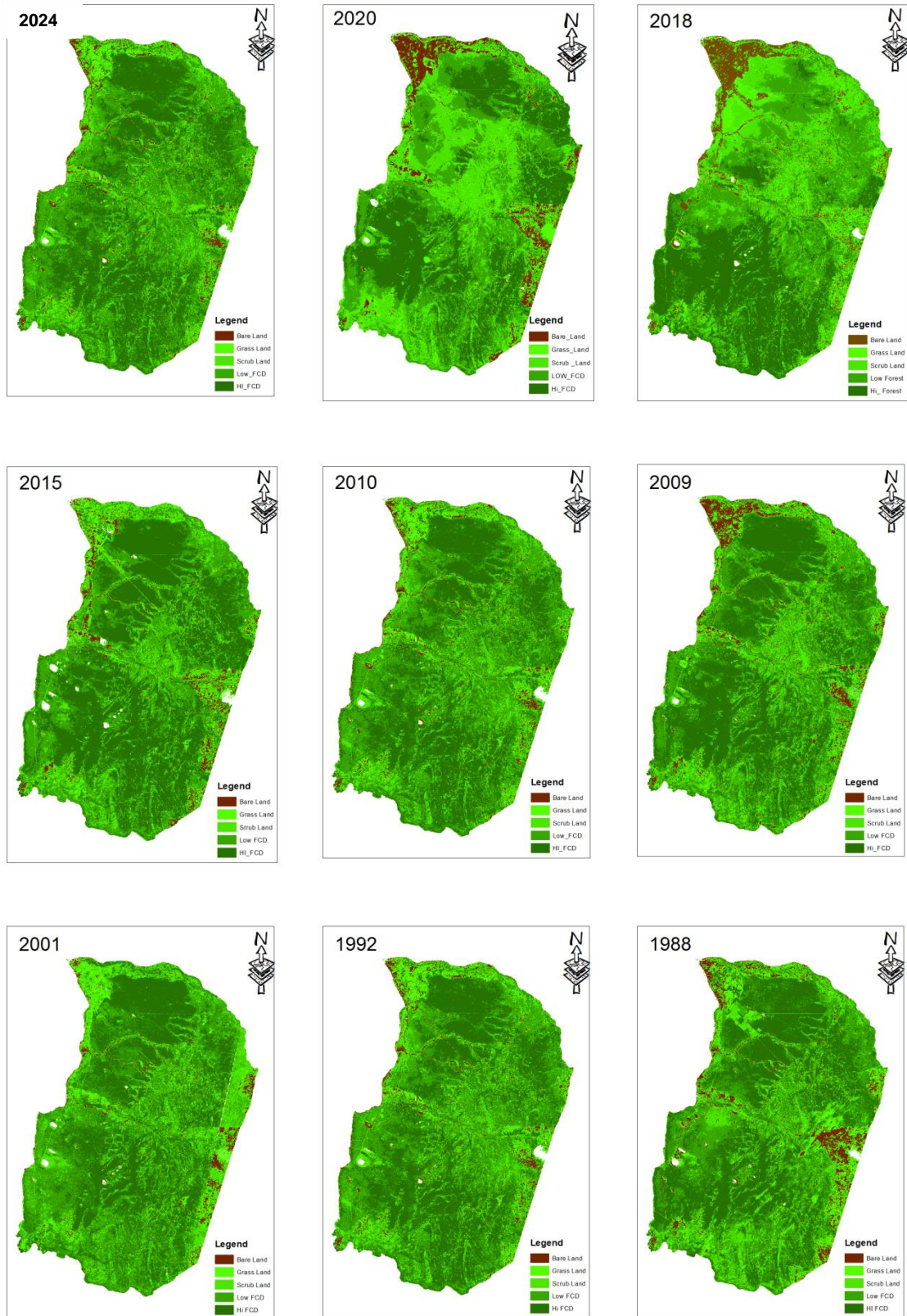


Figure 2.2: Classified FCD Model in to Five Classes for the Years 2024, 2020, 2018, 2015, 2010, 2009, 2001, 1992, and 1988.

3 Results and Discussion

FCD models were derived for the years 1988, 1992, 2001, 2010, 2015, 2018, 2020, and 2024. These FCD models were then classified into five categories: High FCD, Low FCD, Scrub Land, Grass Land, and Bare Land. The next step involved comparing the land area across these classes between the selected years (1988, 1992, 2001, 2009, 2010, 2015, 2018, 2020 and 2024).

3.1 Classification Results of the FCD Model

classification was performed for the developed FCD models of eight selected years, from 1988 to 2020. The models for each year were classified into five classes. The land area and percentage of land area for each class were then calculated for the selected years. figure3.1 presents the results. Notably, the results show a significant drop of approximately 10% in the land area percentage of the High FCD class in 2018, accompanied by a notable increase of about 10% in the Scrub Land class during the same year.

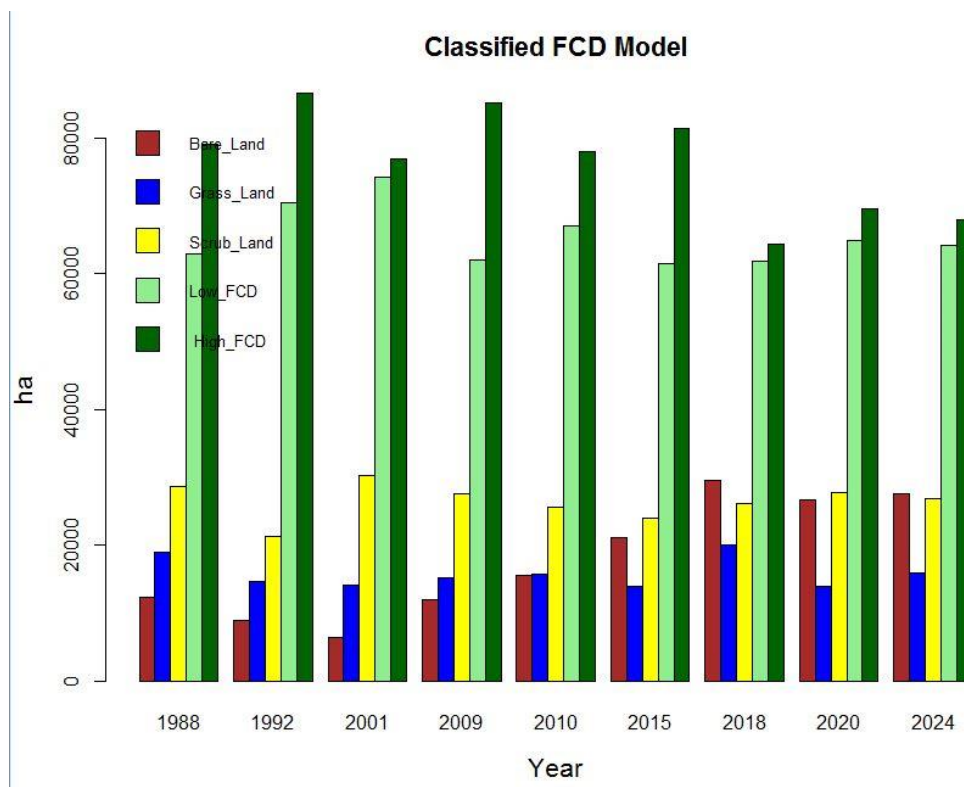


Figure 3.1: FCD Model Classification by Year.

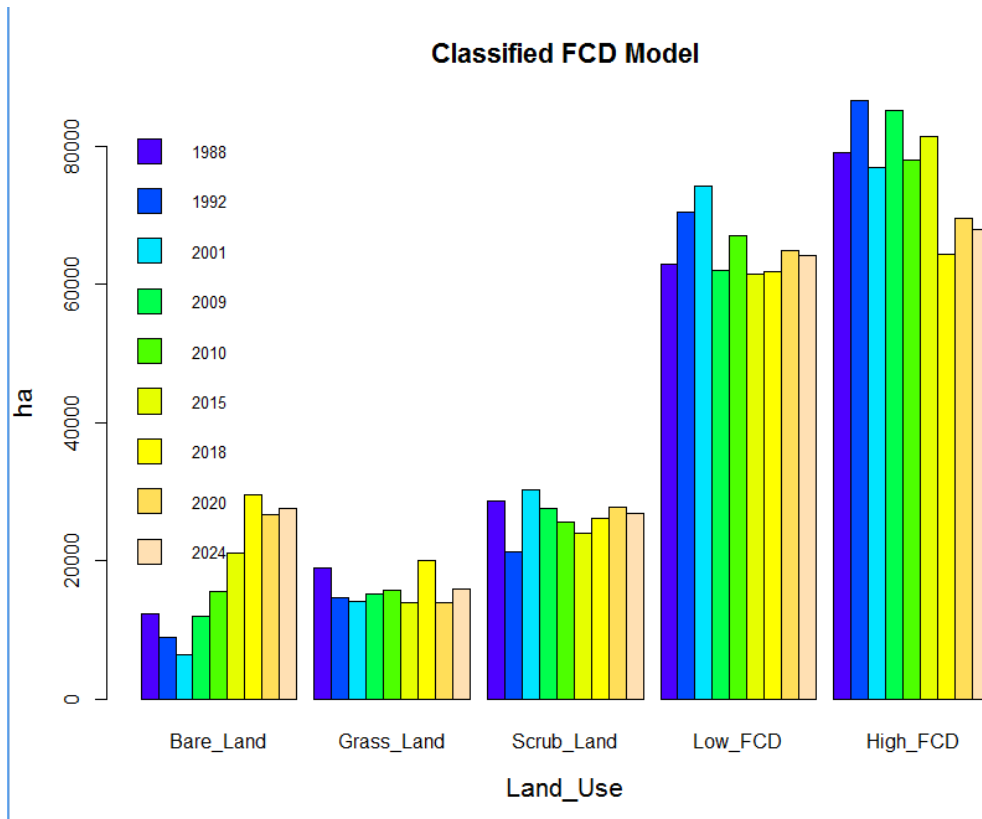


Figure 3.2: FCD Model Classification by Land Use.

The above bar plot chart was constructed (Figure 3.1) representing the land area of each classified classes. This helps to investigate the land use changes on each year. The chart shows and unexpected result as the year 2015 gives comparatively large values for the High-FCD. However, if considered the High-FCD the noticeable declined shows in the year 2018, but no noticeable difference in the other years. The two bar plot charts gives the area wise comparission of different land use classes. The above identified differences of the area of land uses classes were further analysed by overlaying DS division shape file and the GN divition shape files developed by the Survey Department of Sri Lanka on the classified FCD models. This helps to identify major reasons for the changes identified in the bar plot charts.

It was observed a development converting forest area into residential purposes in the Musali divisional secretariat area in Manar district, after overlaying the shape file of DS division on to the created FCD models for the years 2015 to 2020. Further it was identified the GN divisions as Marichchukkadi, Karadikkuli, Poiakuli, Sinnapulachchi, Polkerni and Kandachchi when overlay the GN division shape file on the FCD models of 2011 to 2020.

The development converting forest area into farm land running along the common boarder of the Kondachchi and SinnapullachchiPotkemi GN divisions was observed in the FCD model of 2010. The farm land extends from the above road towards to the Kondachchi GN division for about 1 Km and towards to the SinnapullachciPotkemi for about 700m. This farm land extends towards to the south boarder of the GN division Ahattimurippu from its North and from the south towards to the Kal Aru. This farm land was not clearly visible on the FCD models of 1992, 2001, and 2009. However, a fertile land area like a farm land was clearly observed in the FCD model of 1988.

The human settlement was observed in the area between the coastal boundary and the South Coastal road running through the Kondachchi GN division in the FCD model of 1988. Further, the GN division areas ArippuWest, Arippu East, Poonochchikulam, Veppankulam, Methaveli, Puthuveli, PeriyapullachchiPolkerni, Chilavathurai, Kollankulam, Kokkupadayan were observed as human settlements. the Northern area of the water feature starting from Ahathumurippu tank and running through Ahathumurippu, SinnapilliachchiPotkemi and Maruthamadhu GN divisions towards to the AruviAru were also observed as a human settlement in 1988 FCD model. The small settlement areas were observed in Mullikkulam and Karadikkuli GN divisions western boundary (coastal boundary). The area between ModeragamAru and Northern side of ModaragamAru in Marichchikudi GN division for about 2Km and gradually decrease for about 100m in Palaikuli GN division was also observed as a human settlement according to the 1988 FCD model.

The South coastal road and the Mannar roads were vaguely visible in the developed FCD models of 1992, 2001 and 1988. However, these roads were clearly visible and observed widened in the FCD models after 2009. Further, the road running along the boundary of Kondachchi and SinnapullachchiPotkerni GN division observed widened in the FCD models of 2009 and 2010.

According to the derived FCD models of 2010 and 2011, the human settlement related deforestation activities were visible in Surrounding areas of the Mannar road in Marichchukkaddi and Karadikkuli GN divisions. Further, these activities were observed around 1Km form the boundary of Marichchukkaddi and Palaikuli GN divisions towards the Palaikuli GN division. These settlement activities were also observed around 500m to 600m

surrounded area of Mannar road from the KalAru towards ModaragamAru for about 1.5 Km along the road. The human settlement related deforestation activities were visible towards to the Kondachchi GN division from the South Coastal road for about 300m to 600m.

The human settlement related deforestation activities were visible in the FCD model of year 2015 than that was in the year 2013, specifically the surrounding areas for the South Coastal road. The deforestation activities in surrounding areas of the South Coastal road and the Mannar road were visible in the year 2018 FCD model. The forest area in the FCD model 2020 was greater than that was in the FCD model 2018.

3.2 Identify whether there is a village before the year 1988

There are human settlements in the area before the year 1988. The following can be identified as the human settlements on the created FCD model and the Build Up area Index;

There is a farm land alike surrounding the road running along the common boarder of the Kondachchi and SinnapullachchiPotkemi GN divisions. The farm land extends from the above road towards to the Kondachchi GN division for about 1 Km and towards to the SinnapullachciPotkemi for about 700m. This farm land extends towards to the south boarder of the GN division Ahattimurippu from its North and from the south towards to the KalAru. However, in 1992, this farm land is observed vaguely and vanished afterwards. After the year 2009, it is observed widening of the above road and the re-establishment of the farm land again and the village in the surrounding area of the road.

The human settlement is in the area between the coastal boundary and the South Coastal road running through the Kondachchi GN division. Further, the GN division areas Arippu west, Arippu East, Poonochchikulam, Veppankulam, Methaveli, Puthuveli, PeriyapullachchiPolkerni, Chilavathurai, Kollankulam, Kokkupadayan are human settlements.

The Northern area of the water feature starting from Ahathumurippu tank and running through Ahathumurippu, SinnapilliachchiPotkemi and Maruthamadhu GN divisions towards to the AruviAru are also a human settlement. The small settlement areas are in Mullikkulam and Karadikkuli GN divisions western boundary (coastal boundary).

The area between ModeragamAru and Northern side of ModaragamAru in Marichchikudi GN for about 2Km and gradually decrease for about 100m in Palaikuli GN division is also a human settlement.

3.3 Identify what are the villages established after the year 1988 and in which years

Development of human settlements are identified based on the created FCD model and the Build Up area index. These developments are identified in GN divisions Kondachchi, SinnapullachchiPotkerni, Marichchukkaddi, Karadikkuli and Palaikuli. These all GN divisions are in the Musali DS division. The highest changes are observed in the GN division Palaikuli. The development of the human settlements and the respective years are as follows;

The South coastal road and the Mannar roads are vaguely visible before the year 2009. However, these roads are clearly visible and widened after the year 2009. Further, the road running along the boundary of Kondachchi and SinnapullachchiPotkerni GN division also widened in the period 2009 to 2010.

In the years 2010 and 2011, the human settlement related deforestation activities are visible in Surrounding areas of the Mannar road in Marichchukkaddi and Karadikkuli GN divisions. Further, these activities are observed around 1Km form the boundary of Marichchukkaddi and Palaikuli GN divisions towards the Palaikuli GN division. These settlement activities are also observed around 500m to 600m surrounded area of Mannar road from the KalAru towards ModaragamAru for about 1.5 Km along the road. The human settlement related deforestation activities are visible towards to the Kondachchi GN division from the South Coastal road for about 300m to 600m.

The human settlement related deforestation activities are visible in the year 2015 than that is in the year 2013, specifically the surrounding areas for the South Coastal road. The deforestation activities in surrounding areas of the South Coastal road and the Mannar road are visible in the year 2018 than that is in the year 2015.

However, the resilience of the forest area is visible in the years 2018 to 2020 which indicates the absence of deforestation in the area in this period.

4 Conclusion

Sum of the low and the high FCD values of classified FCD models from the year 1988 to the year 2015 is more than 70%. This value is recorded as 72.9%, 71.8, 70.8% and 69% for the years 2009, 2010, 2015 and 2020 accordingly. However, the value is recorded as 70.2% in the year 1988. This indicates that the true value of the forest area change is 1.2%. In the year 2018 this value is 61.5%. However, In the year 2020 the value observed as 69%. This indicates the significant land cover change from the forest cover towards to the bare or vegetation cover within the period of 2015 to 2018 and from 2018 to 2020 again from bare or vegetation cover to the forest cover. Finally, it can be concluded that these changes are not solely the result of deforestation, but rather a combination of both deforestation and forest degradation.

References

- Azizia, Z., Najafi, A., & Sohrabia, H. (2008). Forest canopy density estimating, using satellite images. In: *The International Archives of the Photogrammetry, Remote Sensing and Spatial Information Sciences*. Vol XXXVII, Part B8, Beijing
- Banerjee, K., Panda, S., Bandyopadhyay, J., & Jain, M. K. (2014). Forest canopy density mapping using advance geospatial technique. *international Journal of innovative science, engineering & technology*, 1(7), 358-363.
- Chang, J., Clay, D. E., Clay, S. A., Chintala, R., Miller, J. M., & Schumacher, T. (2016). Biochar reduced nitrous oxide and carbon dioxide emissions from soil with different water and temperature cycles. *Agronomy Journal*, 108(6), 2214-2221.
- Himayah, S., & Danoedoro, P. (2016, November). The Utilization of Landsat 8 Multitemporal Imagery and Forest Canopy Density (FCD) Model for Forest Reclamation Priority of Natural Disaster Areas at Kelud Mountain, East Java. In IOP Conference Series: *Earth and Environmental Science* (Vol. 47, No. 1, p. 012043). IOP Publishing.

Horning, N. (2004). Land cover classification methods, Version 1.0. American Museum of Natural History, Center for Biodiversity and Conservation. Retrieved from <http://biodiversityinformatics.amnh.org>

Jorge, D. S. F., Amore, D. J., & Barbossa, C. F. (2015). Efficiency estimation of four different atmospheric correction algorithms in a sediment-loaded tropic lake for Landsat 8 OLI sensor. *Proceedings of the Anais XVII Simpósio Brasileiro de Sensoriamento Remoto—SBSR, João Pessoa-PB, Brasil, 25-29.*

Pladsrichuay, S., Suwanwerakamtorn, R., & Pannucharoenwong, N. (2018). Estimating Vegetation Canopy Density in the Lower Chi Basin, Northeast, Thailand Using Landsat Data. *International Journal of Applied Engineering Research*, 13(6), 3215-3219.

Rikimaru, A. (1996). LANDSAT TM Data processing guide for forest canopy density mapping and monitoring model. pp. 1-8. In: *ITTO Workshop on Utilization of Remote Sensing in Site Assessment and Planning for Rehabilitation of Logged-over Forests. Bangkok, Thailand,*

Rikimaru, A., Roy, P. S., and Miyatake, S. (2002). Tropical forest cover density mapping. *Tropical Ecology*. 43(1): 39-47.

Sowmya, D. R., Shenoy, P. D., & Venugopal, K. R. (2017). Remote sensing satellite image processing techniques for image classification: a comprehensive survey. *International Journal of Computer Applications*, 161(11), 24-37.

Ustuner, M., Sanli, F. B., Abdikan, S. A. Y. G. I. N., Esetlili, M. T., & Kurucu, Y. U. S. U. F. (2014). Crop type classification using vegetation indices of rapideye imagery. *The International Archives of Photogrammetry, Remote Sensing and Spatial Information Sciences*, 40(7), 195.

Vermote, E. F., Tanré, D., Deuze, J. L., Herman, M., & Morcette, J. J. (1997). Second simulation of the satellite signal in the solar spectrum, 6S: An overview. *IEEE transactions on geoscience and remote sensing*, 35(3), 675-686.

Weerakoon, D K and WLDPTS de A Goonatilake (2007) Diversity of Avifauna in the Vilpattu National Park. Retrieved from <https://www.researchgate.net/publication/299823094>

Wilpattu National Park. (n.d.). retrieved from <https://amazinglanka.com/>(25 June 2019).

Wu, C., Shen, H., Wang, K., Shen, A., Deng, J., & Gan, M. (2016). Landsat imagery-based above ground biomass estimation and change investigation related to human activities. *Sustainability*, 8(2), 159.

Xue, J., & Su, B. (2017). Significant remote sensing vegetation indices: A review of developments and applications. *Journal of sensors*, 2017.